



## Structural characterization and antioxidant activities of polysaccharides from *Citrus aurantium* L.



Qiu Hong Wang<sup>1</sup>, Zun Peng Shu<sup>1</sup>, Bing Qing Xu, Na Xing, Wen Juan Jiao, Bing You Yang, Hai Xue Kuang\*

Key Laboratory of Chinese Materia Medica (Heilongjiang University of Chinese Medicine), Ministry of Education, Harbin 150040, China

### ARTICLE INFO

#### Article history:

Received 20 January 2014

Received in revised form 25 February 2014

Accepted 2 March 2014

Available online 12 March 2014

#### Keywords:

*Citrus aurantium* L.

Polysaccharide

Structural characterization

Antioxidant activity

### ABSTRACT

Three polysaccharide fractions were obtained from *Citrus aurantium* L. (CAL) by sequential extraction with cold water, hot water, and 1.0 M NaOH, respectively. The fractions were denoted CALA, CALB, and CALC. Structural characterization was conducted by physicochemical property, FTIR, and SEM analyses. Antioxidant activities in vivo and in vitro were also evaluated. CALB, which showed the highest activity, was further isolated to afford four purified polysaccharides (CALB-1–4) by various ion exchange and gel-filtration chromatography. Meanwhile, the purified polysaccharides were subjected to composition analysis and screened by antioxidant activity in vitro. Among the four purified polysaccharides, CALB-3 had the highest antioxidant activity and its structure was analyzed by FTIR, SEM and AFM microscopy. Overall, these results indicated that polysaccharides from CAL had potential therapeutic applications in the medical and food industries because of their antioxidant activities.

© 2014 Elsevier B.V. All rights reserved.

## 1. Introduction

*Citrus aurantium* L. (CAL) and *Citrus sinensis* Osbeck, the main botanical origins of the famous traditional Chinese medicine *Fructus aurantii* (*Zhi-qiao*), have been used for thousands of years [1]. *Zhi-qiao* is extensively used in clinics in China, Korea, Japan, and other Asian countries to treat fullness of the gastrohelcosis [2] and ischemia [3]. Many traditional Chinese medicine preparations containing *Zhi-qiao* are available, including *Zhizhu Wan*, *Fufang Dachengji Tang*, and *Fufang Changweining* [2]. Given its medicinal importance, the demand for *Zhi-qiao* has steadily increased.

The search for natural sources of polysaccharide has intensified because of a wide range of biological properties, its low toxicity, and few side effects. Antioxidant [4], immunomodulation [5], anti-tumor [6], anti-virus [7], anti-complementary [8], and anti-inflammatory activities [9] have been exhibited by many polysaccharides extracted from medicinal fungi and plants. Plants, particularly those used as traditional Chinese medicines, contain high amounts of natural plant polysaccharides.

To date, studies on *Zhi-qiao* mainly focus on low molecular-weight substances, such as various flavonoids and flavone glycosides, whereas less attention has been focused on polysaccharides because they belong to high molecular-weight compounds. However, in our studies, polysaccharides of *Zhi-qiao* have been identified as free radical or active oxygen scavengers. Few scientific reports are available in literature on the isolation, purification, and bioactivity determination of polysaccharides from *Zhi-qiao*, especially detailed studies on antioxidant activities and chemical composition.

Herein, polysaccharides from *Zhi-qiao* were first sequentially extracted using cold water, hot water, and 1.0 M NaOH. The preliminary structural characterization of the three polysaccharides was then conducted via physicochemical property, FTIR, and SEM analyses. Antioxidant activities of the three polysaccharides via in vivo and in vitro processes were also evaluated. Finally, the active polysaccharide fraction (CALB) was further isolated, purified, and its chemical composition was analyzed. Among the four purified polysaccharides, CALB-3 had the highest antioxidant activity and its structure was elucidated by FTIR, SEM and AFM microscopy.

## 2. Materials and methods

### 2.1. Plant materials

The dry immature fruits of *C. aurantium* L. were collected in May 2010 from Xingan of Jiangxi Province, China and identified by Prof.

\* Corresponding author at: Heilongjiang University of Chinese Medicine, No. 24, Heping Road, 11 Xiangfang District, Harbin 150040, China. Tel.: +86 451 82193001; fax: +86 451 82110803.

E-mail address: [hxkuang@hotmail.com](mailto:hxkuang@hotmail.com) (H.X. Kuang).

<sup>1</sup> These authors contributed equally to the study.

Zhenyue Wang, a pharmacognosist from the Department of Pharmacognosy, School of Pharmacy, Heilongjiang university of TCM (Harbin China). The voucher specimen (20100018) was deposited at herbarium of Heilongjiang University of Chinese Medicine, Harbin, P.R. China.

## 2.2. Chemicals and reagents

2,2-Diphenyl-1-picryl-hydrazyl (DPPH) were purchased from the Sigma Chemical Co. (St. Louis, MO, USA). Ascorbic acid (VC), nitro blue tetrazolium (NBT), and nicotinamide adenine dinucleotide-reduced (NADH) were purchased from the Sinopharm Chemical Reagent Co. (Beijing, China). DEAE-52 cellulose was purchased from Whatman International Ltd. (Maidstone, Kent, UK), and DEAE-Sepharose Fast Flow, Sephacryl S-400 HR were purchased from the Pharmacia Co. (Sweden). The kits for determining malondialdehyde (MDA) contents, glutathione peroxidase (GSH-Px), catalase (CAT), and superoxide dismutase (SOD) activity were obtained from Jiancheng Bioengineering Institute (Nanjing, China). All reagents were analytical grade, or were the highest grade available.

## 2.3. Animals

Male C57BL/6N (weighing 17–18 g, aged 6 weeks), provided by the Experimental Animal Center of Medical Department of Peking University were used in this study. The mice were kept in a temperature controlled facility (temperature:  $22 \pm 1^\circ\text{C}$ , humidity: 60%) with a 14 h light/10 h dark photo-period, and free access to food and water. Animal welfare and experimental procedures were carried out strictly in accordance with the guide for the care and use of laboratory animals (The Ministry of Science and Technology of China, 2006) and the related ethical regulations of our university. All efforts were made to minimize animal's suffering and to reduce the number of animals used.

## 2.4. Extraction and isolation of crude polysaccharides and identification on purity of polysaccharides

The dry immature fruits of *C. aurantium* L. were knocked into small pieces, and submitted to sequential extractions as follows: small pieces (1.0 kg) were refluxed with 5 vol. of 95% ethanol 3 times for 2 h each time. The residue was dried in air and then extracted 3 times with 5 vol. of distilled water for 24 h (each time) at  $4^\circ\text{C}$ . The combined aqueous extracts were filtered, concentrated 10-fold, and 95% EtOH added to final concentration of 80%. The precipitate was dissolved in 600 mL of water and deproteinated 9 times with 200 mL of 5:1 chloroform-*n*-butanol as described by Staub. The resulting aqueous fraction was extensively dialyzed (cut-off Mw 3500 Da) against tap water for 48 h and distilled water for 48 h and precipitated again by adding a 5-fold volume of ethanol. After centrifugation, the precipitate was washed with anhydrous ethanol and then dissolved in water and lyophilized to yield the crude polysaccharide A (32 g) was collected by centrifugation (3000 rpm, 10 min,  $20^\circ\text{C}$ ). A similar procedure was used with 10 vol. of hot water ( $100^\circ\text{C}$ , 2 h,  $5\times$ ) and 1 M sodium hydroxide solutions ( $4^\circ\text{C}$ , 8 h,  $5\times$ ) for above the residue after cold water extraction. The fractions obtained were labeled crude polysaccharides B (177 g) and C (30 g). The yields of three crude polysaccharides were 3.2%, 17.7% and 3% of the plant raw material, respectively [10].

Crude polysaccharide B (5 g) was dissolved in distilled  $\text{H}_2\text{O}$  and passed through two series connected resin columns (Amberlite FPA90-Cl ( $\text{Cl}^-$  form) and Amberlite FPC3500 ( $\text{H}^+$  form)) eluting with distilled  $\text{H}_2\text{O}$ , 0.5 M NaCl solution and 1.0 M NaCl solution to yield fractions Fr. B1 (2.1 g), Fr. B2 (1.4 g), and Fr. B3 (0.3 g), respectively. Fr. B1 was chromatographed over DEAE-Sepharose Fast Flow

eluting with distilled water, 0.1 M NaCl solution and 0.3 M NaCl solution to yield subfractions Fr. I, Fr. II, and Fr. III, respectively. Fr. I (421.5 mg) and Fr. II (986.0 mg) were further purified by gel-permeation chromatography on a high resolution Sephacryl S-400 eluting with distilled water to afford CALB-1 (302.4 mg) (Fig. 3A) and CALB-2 (783.6 mg) (Fig. 3B), respectively. Fr. B2 was applied to a DEAE-cellulose 52 column with 0.5 M and 1 M NaCl solution to afford CALB-3 (284.0 mg) (Fig. 3C) and CALB-4 (419.1 mg) (Fig. 3D). Polysaccharides in the eluted fractions were detected using the phenol-sulfuric acid method and all NaCl elute fractions in column chromatography were dialyzed against distilled water for 48 h (cut-off Mw 3500 Da) and then freeze-dried, and the yields of four purified polysaccharides were 6.048%, 15.672%, 5.68%, and 8.382% for CALB-1, CALB-2, CALB-3, and CALB-4 of the parent crude polysaccharide B by ion exchange and gel-filtration chromatography, respectively.

Purity of the four polysaccharides ( $2\text{ mg mL}^{-1}$ ) was determined by high performance liquid chromatography (HPLC), using Waters 2695 HPLC and Alltech ELSD 2000 detector. The separation was carried out on a Shodex sugar KS-805 column ( $8.0\text{ mm} \times 300\text{ mm}$ ,  $17\text{ }\mu\text{m}$ ) coupled with a Shodex KS-G guard column ( $6\text{ mm} \times 50\text{ mm}$ ,  $7\text{ }\mu\text{m}$ ). The isocratic elution was employed using water with  $0.5\text{ mL/min}$  at  $30^\circ\text{C}$  and the injection volume was  $10\text{ }\mu\text{L}$ . While the drift tube temperature for ELSD was set at  $110^\circ\text{C}$ , the nitrogen flow rate was  $3.3\text{ L/min}$  for the determination of polysaccharides. Their purities were over 98% by HPLC analysis.

## 2.5. Physicochemical property analysis

Physicochemical properties were determined using the following methods: shape observation, color observation, solubility test,  $\text{FeCl}_3$  reaction,  $\alpha$ -naphthol reaction, iodination reaction, Fehling's test, phenol-sulfuric acid reaction, sulfuric acid carbazole reaction, Coomassie brilliant blue reaction and full wavelength scanning. Total carbohydrate contents in three crude polysaccharides were determined by phenol-sulfuric acid colorimetric method (490 nm) using glucose as the standard. Uronic acid contents and protein contents in three crude polysaccharides were determined by sulfuric acid carbazole reaction (530 nm) and Coomassie brilliant blue reaction (595 nm), respectively.

## 2.6. FTIR analysis

The organic functional groups of three polysaccharides were identified using an FTIR spectrophotometer (FTIR-8400S, Shimadzu Co., Japan) within  $4000\text{--}400\text{ cm}^{-1}$  via the KBr pressed-disk method.

## 2.7. Molecular morphology analysis

The three polysaccharides were coated with a thin layer of gold under reduced pressure. They were then examined using a SEM system (Apollo 300, CamScam, UK) at a 10 kV acceleration voltage, as well as image magnifications of  $1000\times$  and  $3000\times$ .

The atomic force microscopy in this study was manufactured by Harbin Institute of Technology (Harbin, China) and operated in the tapping mode. CALB-3 was diluted to the final concentration of  $10\text{ }\mu\text{g/mL}$  in distilled water.  $5\text{ }\mu\text{L}$  of solutions was dropped onto freshly cleaved mica and allowed to stand in air before imaging.

## 2.8. Analysis of monosaccharide composition

The procedure of analyzing monosaccharide composition was described as follows: polysaccharide sample (10 mg) was dissolved in 2 mL of 2.0 M TFA (trifluoroacetic acid) in an ampoule (5 mL). The ampoule was sealed under a nitrogen atmosphere and kept in

120 °C to hydrolyze the polysaccharide into component monosaccharides for 160 min and cooled down. The reaction mixture was added methanol and vacuum distilled to remove the rest TFA. Then the dry residuum was dissolved in double distilled water (1.4 mL) and derived as following experiments. PMP derivatization of monosaccharides was placed in the 7.0 mL centrifuge tubes, then 0.5 M methanol solution (700  $\mu$ L) of PMP and 0.3 M aqueous sodium 5 hydroxide (700  $\mu$ L) were added to every tube. Each mixture was placed at 70 °C water bath for 60 min, then cooled to room temperature and neutralized with 700  $\mu$ L of 0.3 M HCl. The resulting solution was performed on liquid–liquid extraction with same volume of isoamyl acetate (two times) and chloroform (one time), respectively. The isoamyl acetate or chloroform solution layer was carefully removed after being shaken vigorously and centrifuged. Then the aqueous-methanol layer was filtered through a 0.45  $\mu$ m membrane and diluted with water before HPLC analysis. The above derivatized method was performed to the mixed standard monosaccharides which include D-mannose, L-rhamnose, D-glucose, D-galactose, L-arabinose, D-xylose, D-ribose, D-glucuronic acid, and D-galacturonic acid. The derivatization procedure of hydrolysate samples and standard samples must be carried out simultaneously under the same condition.

The analysis of PMP-derived monosaccharides was carried out by Waters 2695 HPLC and Waters 2996 detector, a breeze station was used to perform the data collection. Separation was carried out in a TSKgel ODS-100V (4.6 mm  $\times$  25 mm, 5  $\mu$ m). The molar ratio of the component monosaccharides is calculated as follows: the correction factor is shown in the equation:  $f_i/n = (m_i/A_i)/(m_n/A_n)$ , where  $A_i$  and  $A_n$  are the values of their peak areas in the standard monosaccharide, respectively.  $m_i$  and  $m_n$  are the values of their weights of the standard monosaccharide, respectively. The molar ratio value is shown in the equation:  $R_{i/n} = f_{i/n} \times (A_i/A_n)$ , where  $A_i/A_n$  is the ratio value of peak area for the component monosaccharide of tested samples and  $f_{i/n}$  is the correction factor.

## 2.9. Antioxidative activities

### 2.9.1. Antioxidative activities in vitro

**2.9.1.1. DPPH radical scavenging activity.** The DPPH radical scavenging activity was determined according to the method described by [11] with some modifications. The three polysaccharides were dissolved in water, yielding a series of sample solutions with different concentrations (0.20, 0.40, 0.80, 1.6, 3.2, and 6.4 mg mL<sup>-1</sup>). A sample solution (2 mL) was mixed with 2 mL of 0.20 mM DPPH–ethanol solution, and the absorbance of the sample solution ( $A_{\text{sample}}$ ) was measured at 517 nm against a blank after 60 min. The absorbance of the DPPH–ethanol solution ( $A_{\text{DPPH}}$ ) was also measured at 517 nm. The DPPH radical scavenging capability was calculated using the following equation:

$$\text{DPPH radical scavenging activity (\%)} = \left[ \frac{A_{\text{DPPH}} - A_{\text{sample}}}{A_{\text{DPPH}}} \right] \times 100$$

where  $A_{\text{DPPH}}$  is the absorbance of the control only without samples or standard sample and  $A_{\text{sample}}$  is the absorbance of samples or standard sample.

**2.9.1.2. Hydroxyl radical scavenging activity.** Scavenging activity against hydroxyl radical was determined according to Fenton's reaction [12]. The three polysaccharides were dissolved in water, yielding a series of sample solutions with different concentrations (0.20, 0.40, 0.80, 1.6, 3.2, and 6.4 mg mL<sup>-1</sup>). A mixture solution was prepared by mixing several solutions into 2 mL of PBS (pH 7.4) in the following order: 1 mL of water, 1 mL of 1,10-phenanthroline ethanol solution (0.75 mM), 1 mL of FeSO<sub>4</sub> (0.75 mM), and 1 mL of H<sub>2</sub>O<sub>2</sub> (0.01%). The final mixture was incubated for 60 min at 37 °C

and was used as the blank solution. A similar procedure was used to prepare the control solution, wherein 1 mL of water instead of H<sub>2</sub>O<sub>2</sub> was added. The absorbance rates of the blank ( $A_{\text{blank}}$ ), control ( $A_{\text{control}}$ ), and sample solutions ( $A_{\text{sample}}$ ) were recorded at 510 nm. Hydroxyl radical scavenging activity was calculated using the following equation:

Hydrogen peroxide scavenging activity (%)

$$= \left[ \frac{A_{\text{control}} - A_{\text{sample}} + A_{\text{blank}}}{A_{\text{control}}} \right] \times 100$$

where  $A_{\text{control}}$  is the absorbance of control sample (water instead of sample),  $A_{\text{sample}}$  is the absorbance in the presence of tested sample, and  $A_{\text{blank}}$  is the absorbance of the sample only (water instead of H<sub>2</sub>O<sub>2</sub> solution).

**2.9.1.3. Superoxide radical scavenging activity.** Superoxide radical scavenging activity was determined according to the NBT reduction method [13]. The three polysaccharides were dissolved in water, yielding a series of sample solutions with different concentrations (0.20, 0.40, 0.80, 1.6, 3.2, and 6.4 mg mL<sup>-1</sup>). The reaction mixture containing 1.5 mL of sample solution, 0.50 mL of 300  $\mu$ M NBT, 0.50 mL of 468  $\mu$ M NADH, and 0.50 mL of 60  $\mu$ M PMS were incubated at 25 °C for 5 min. The absorbance was recorded at 560 nm against a blank, wherein the sample was replaced by PBS. Superoxide radical scavenging activity was calculated using the following equation:

Superoxide radical scavenging activity (%)

$$= \left[ \frac{A_{\text{control}} - A_{\text{sample}}}{A_{\text{control}}} \right] \times 100$$

where  $A_{\text{control}}$  is the absorbance of the control only without samples or standard sample and  $A_{\text{sample}}$  is the absorbance of samples or standard sample.

**2.9.1.4. H<sub>2</sub>O<sub>2</sub> scavenging activity.** H<sub>2</sub>O<sub>2</sub> scavenging activity was determined according to the method decided by Gülçin [14] with some modifications. The three polysaccharides and H<sub>2</sub>O<sub>2</sub> were dissolved in 0.1 mol/L of phosphate buffered solution, yielding a series of sample solution and 20 min at a standstill. The absorbance rates of the blank, control, and sample solutions were recorded at 510 nm. H<sub>2</sub>O<sub>2</sub> scavenging activity was calculated using the following equation:

$$\text{H}_2\text{O}_2 \text{ scavenging activity (\%)} = \left[ \frac{A_{\text{control}} - A_{\text{sample}} + A_{\text{blank}}}{A_{\text{control}}} \right] \times 100$$

where  $A_{\text{control}}$  is the absorbance of control sample (water instead of sample),  $A_{\text{sample}}$  is the absorbance in the presence of tested sample, and  $A_{\text{blank}}$  is the absorbance of the sample only (water instead of H<sub>2</sub>O<sub>2</sub> solution).

### 2.9.2. Antioxidative activities in vivo

**2.9.2.1. Experimental design for an aging model induced by D-galactose.** Experimental Design for an Aging Model Induced by D-galactose. C57 mice were randomly divided into 12 groups of 12 mice each. The groups were categorized as normal, model, positive control, and three polysaccharide administration groups. The normal group was administered with 0.2 mL of normal saline s.c., and 0.5 mL of water p.o. daily. The model group was administered with 0.2 mL of 140 mg/kg D-galactose s.c., and 0.5 mL of water p.o. daily. The positive control group was administered with 0.2 mL of 140 mg/kg D-galactose s.c., and 0.5 mL of 100 mg/kg vitamin C p.o. daily. The three polysaccharide administration groups were administered with 0.2 mL of 140 mg/kg D-galactose s.c., and 0.5 mL of 50,

100, and 200 mg/kg polysaccharide p.o. daily, respectively. All mice were successively administered with the above concoctions for 45 d.

**2.9.2.2. Analysis of the expression levels of endogenous antioxidant enzymes and MDA.** To determine the anti-oxidation mechanisms of three polysaccharide, its effects on antioxidant-related endogenous enzymes (i.e., SOD, GSH-Px, and CAT) and the lipid peroxidation metabolic product MDA were investigated. Blood samples were collected from the orbital venous plexuses of the mice under anesthesia. The hearts and livers were rapidly excised and thoroughly washed to clear off blood. The tissues were immediately transferred to ice-cold saline and homogenized (10%) in cold saline (about 4 °C). The blood and homogenate tissues were centrifuged at  $3000 \times g$  and 4 °C for 20 min. SOD, GSH-Px, CAT, and MDA in the supernatants were assessed using the respective detection kits as previously reported by [15].

### 2.10. Statistical analysis

All the experiments were carried out in triplicate, and the data was expressed as the mean standard deviation of the means (S.D.) and statistical analysis was performed by paired samples *t*-test using SPSS 16.0 to evaluate the significance of differences between groups.

**Table 1**

Comparison of the physicochemical properties of the three polysaccharides.

Method	CALA	CALB	CALC
Shape observation	Sheet	Power	Power
Color observation	Taupe	Taupe	Dark brown
Solubility test	Water soluble	Water soluble	Alkali soluble
FeCl <sub>3</sub> reaction	(–)	(–)	(–)
$\alpha$ -Naphthol reaction	(+) <sup>a</sup>	(+)	(+)
Iodination reaction	(–) <sup>b</sup>	(–)	(–)
Fehling's test	(–)	(–)	(–)
Phenol–sulfuric acid reaction	(+)	(+)	(+)
Sulfuric acid carbazole reaction	(–)	(–)	(–)
Coomassie brilliant blue reaction	(+)	(+)	(+)

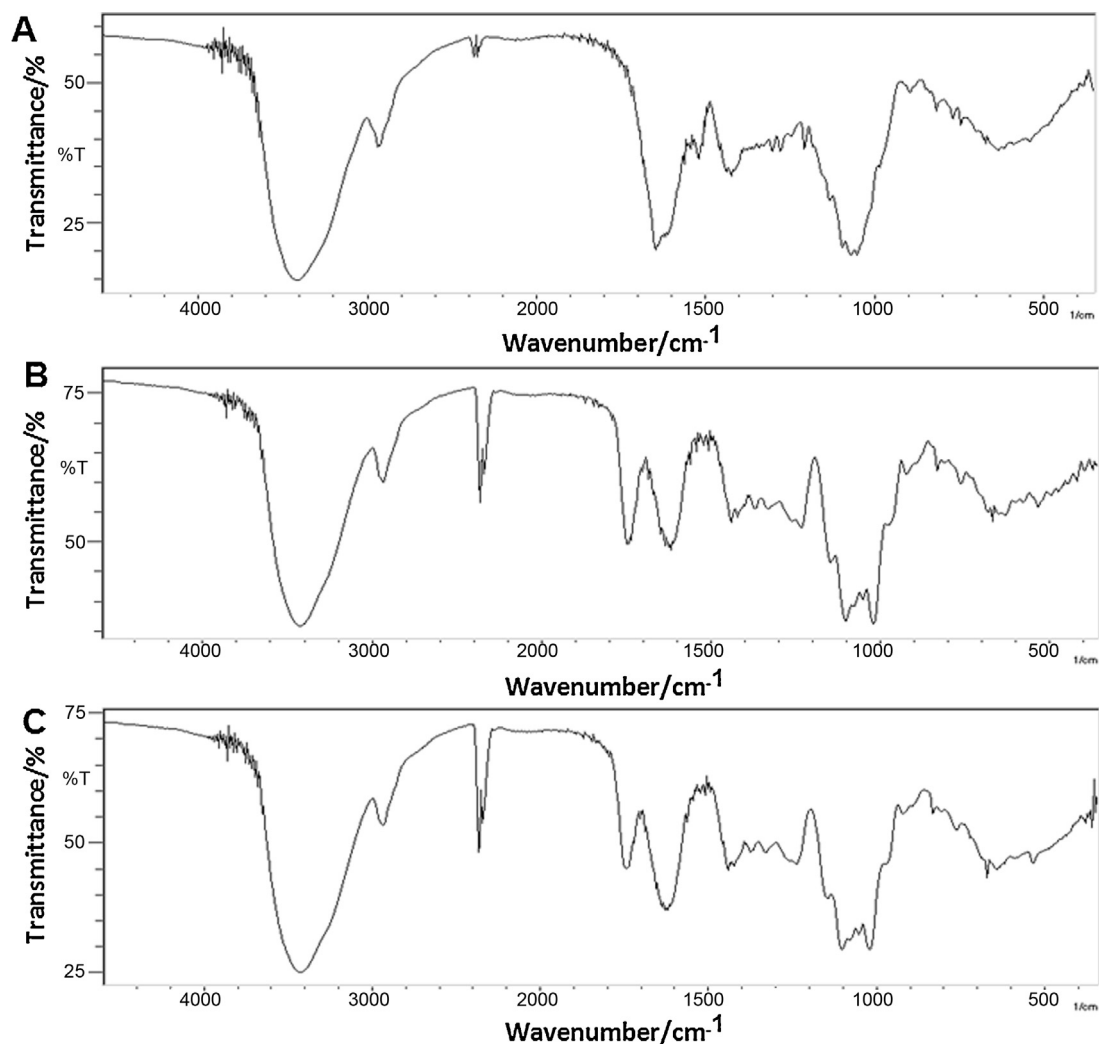
<sup>a</sup> Positive.

<sup>b</sup> Negative.

## 3. Results

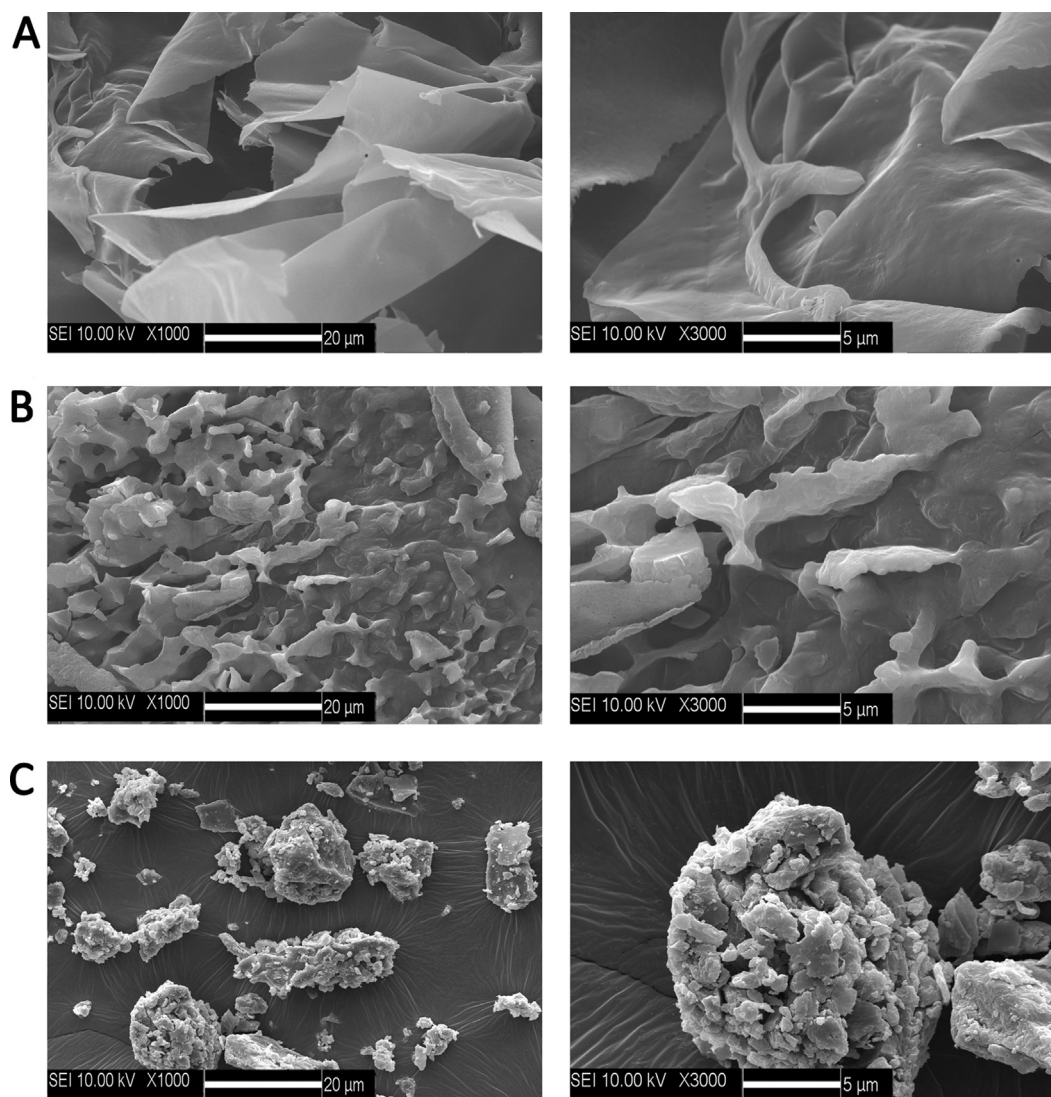
### 3.1. Physicochemical property analysis

Table 1 lists the physicochemical properties of the three polysaccharides. The shape of the three polysaccharides extracted sequentially by different methods had few differences. CALB and CALC were both in powdered form, whereas CALA formed sheets, respectively. CALC was dark brown, whereas the others were taupe. In the test of solubility, CALA and CALB have good solubility in



**Fig. 1.** Infrared spectra of the three polysaccharides. (A) CALA; (B) CALB; (C) CALC.





**Fig. 2.** Scanning electron micrographs of the three polysaccharides. (A) CALA (1000 $\times$ ), (3000 $\times$ ); (B) CALB (1000 $\times$ ), (3000 $\times$ ); (C) CALC (1000 $\times$ ), (3000 $\times$ ).

water and high solubility in hot water, whereas CALC was alkali-soluble. Results of the iodination reaction and Fehling's test indicate that all three polysaccharides did not contain reducing sugar and starch-type polysaccharide. Biuret reaction, Coomassie brilliant blue reaction, phenol sulfuric acid reaction,  $\text{FeCl}_3$  reaction, sulfuric acid carbazole reaction, and  $\alpha$ -naphthol reaction were similar for the three polysaccharides. These similarities indicated that the three extracts were polysaccharides and contained some proteins and uronic acid but did not contain starch and polyphenol.

Total carbohydrate contents in the three crude polysaccharide extracts were determined by phenol–sulfuric acid colorimetric method using glucose as the standard. Uronic acid and protein contents in the three crude polysaccharide extracts were determined by sulfuric acid carbazole reaction and Coomassie brilliant blue reaction, respectively. The results of the phenol–sulfuric acid reaction, sulfuric acid carbazole reaction, and Coomassie brilliant blue reaction are shown in Table 2. Polysaccharide content in the three crude polysaccharide contents were 76.74%, 81.35%, and 71.36% by reference to the calibration curve ( $y = 7.8951x + 0.0057$ ,  $r^2 = 0.9995$ ) plotted from a series of standard glucose solution of known concentration (0.1, 0.05, 0.025, 0.0125, and 0.00625  $\text{mg mL}^{-1}$ ). Uronic acid content in the three crude polysaccharide extracts were 53.11%, 48.76%, and 88.24% by reference to the calibration curve

( $y = 4.6176x - 0.0583$ ,  $r^2 = 0.9989$ ) plotted from a series of standard uronic acid solution of known concentration (0.4, 0.2, 0.1, 0.05, and 0.025  $\text{mg mL}^{-1}$ ). Protein content in the three crude polysaccharide extracts were 21.41%, 17.01%, and 24.64% by reference to the calibration curve ( $y = 0.8223x + 0.0135$ ,  $r^2 = 0.9992$ ) plotted from a series of standard protein solution of known concentration (0.1, 0.2, 0.3, 0.4, 0.5, and 0.6  $\text{mg mL}^{-1}$ ).

### 3.2. FTIR analysis

FTIR spectroscopy is typically used for the qualitative measurement of organic functional groups, especially O–H, N–H, and

**Table 2**

The polysaccharide content, uronic acid content, and protein content in three crude polysaccharides.

	Polysaccharide content (%)	Uronic acid content (%)	Protein content (%)
CALA	76.74	53.11	21.41
CALB	81.35	48.76	17.01
CALC	71.36	88.24	24.64

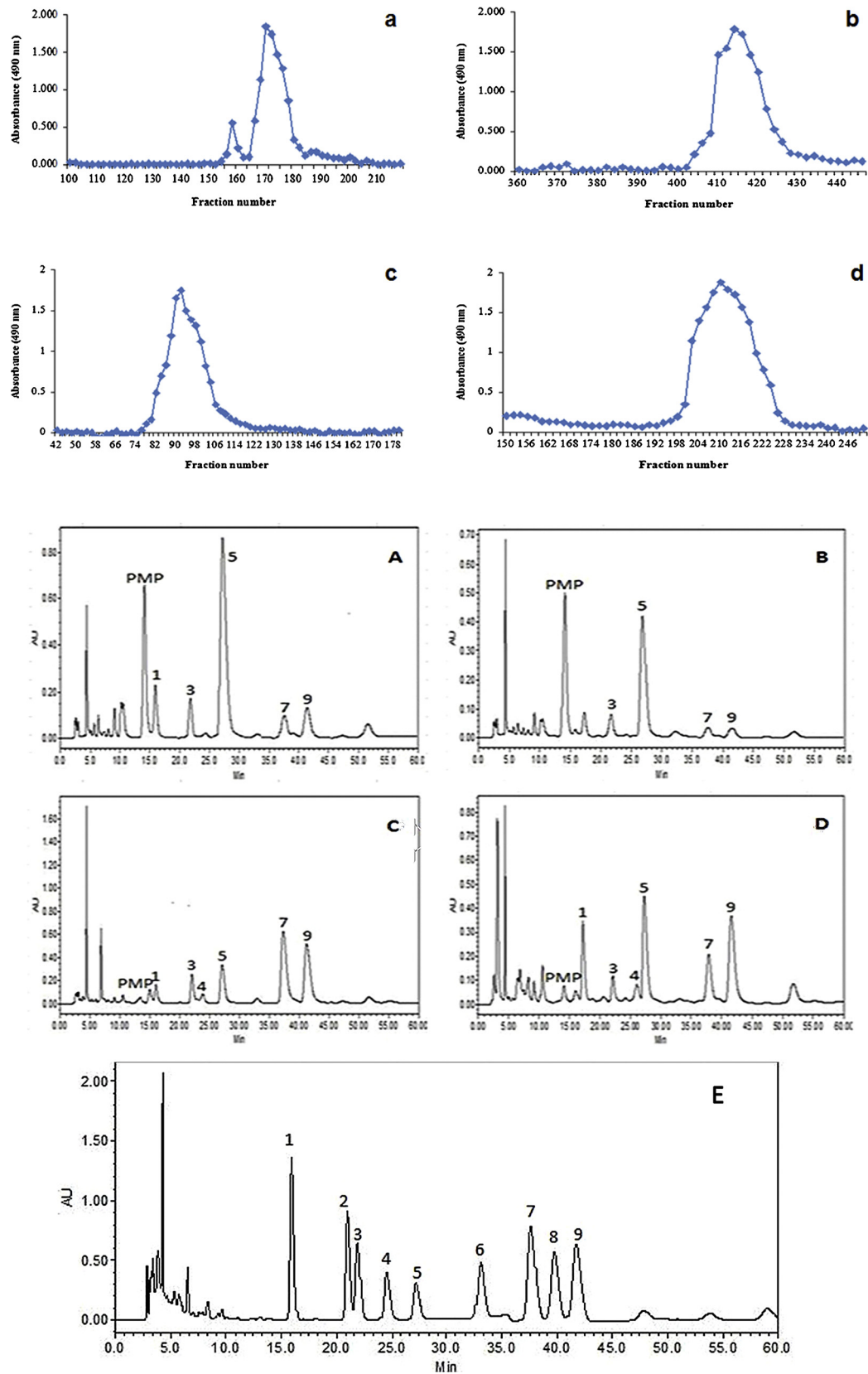


**Fig. 3.** (a–d) Chromatography of four purified polysaccharides (CALB-1–4). (A–D) Electropherograms of PMP derivatives of monosaccharides in four purified polysaccharides; (E) electropherograms of PMP derivatives of 9 standard monosaccharides.

C=O [16]. Fig. 1 shows the FTIR spectra of the three polysaccharides from CAL. Stretching vibration of O–H, saturated C–H, and C–O was observed at 3300–3500, 2929–2989, and 1744  $\text{cm}^{-1}$ , respectively. The absorption bands at approximately 1640 and 1540  $\text{cm}^{-1}$  were attributed to amides I and II, which indicate that the three polysaccharides had conjugated proteins. The absorption band at 1000–1200  $\text{cm}^{-1}$  suggested that the three polysaccharides contained C–O–C or C–O–H in their structures. An absorbance at approximately 880  $\text{cm}^{-1}$  strongly suggested the linkage of  $\beta$ -glycosides in the molecular structure of the three polysaccharides. In conclusion, no significant difference was observed in the FTIR of the three polysaccharides and FTIR spectroscopy did not clearly distinguish the three polysaccharides from each other.

### 3.3. SEM analysis

The SEM images of the three sequential polysaccharide extracts are shown in Fig. 2. Results showed that the different extraction methods induced different physical changes. Fig. 2A shows that CALA had a thin slice shape and the surface was very smooth. Fig. 2B shows that CALB had a rough surface like clouds with characteristic large wrinkles. Fig. 2C shows that CALC was group-like and was composed of many small particles. In summary, the three polysaccharides from CAL by sequential extraction were qualitatively identified by comparing their micrographs with those of standards.

### 3.4. Identification on purity of polysaccharides

The four purified polysaccharides exhibited only a single and symmetrical sharp peak in the phenol–sulfuric acid colorimetric method (UV757CRT, Jingke, Shanghai) (Fig. 3a–d) and high-performance gel-permeation chromatography by HPLC–ELSD with Shodex sugar KS-805 column (data not show).

### 3.5. Analysis of monosaccharide composition

As shown in Fig. 3A–D, PMP derivatives of the component monosaccharides released from the four purified polysaccharides could still be perfectly baseline-separated from each other and the component monosaccharides could be identified by comparison of the chromatogram of the mixture of standard monosaccharides. CALB-1 was composed of Man, Rha, GalUA, Gal, and Ara and their corresponding molar percentages (mol%) were 15.6%, 7.5%, 42.2%, 14.4%, and 20.3%, respectively. CALB-2 was composed of Rha, GalUA, Gal, and Ara and their corresponding molar percentages (mol%) were 12.3%, 49.4%, 21.5%, and 16.8%, respectively. CALB-3 was composed of Man, Rha, GlcUA, GalUA, Gal, and Ara and their corresponding molar percentages (mol%) were 4.2%, 4.5%, 1.7%, 6.1%, 45.8%, and 37.8%, respectively. CALB-4 was composed of Man, Rha, GlcUA, GalUA, Gal, and Ara and their corresponding molar percentages (mol%) were 16.3%, 4.0%, 2.9%, 13.4%, 21.7%, and 41.7%, respectively.

### 3.6. Antioxidative activities

#### 3.6.1. Antioxidative activities in vitro

**3.6.1.1. DPPH radical scavenging activity.** Antioxidants transfer either an electron or a hydrogen atom to DPPH upon interacting with DPPH, thus neutralizing its free radical characteristic. Fig. 4A shows the scavenging activities of CALA, CALB, CALC, and VC against the DPPH radical. The scavenging effects of the three polysaccharides were evidently in a dose-dependent manner. CALA had the weakest activity. At 6.4  $\text{mg mL}^{-1}$ , the scavenging activities of CALA,

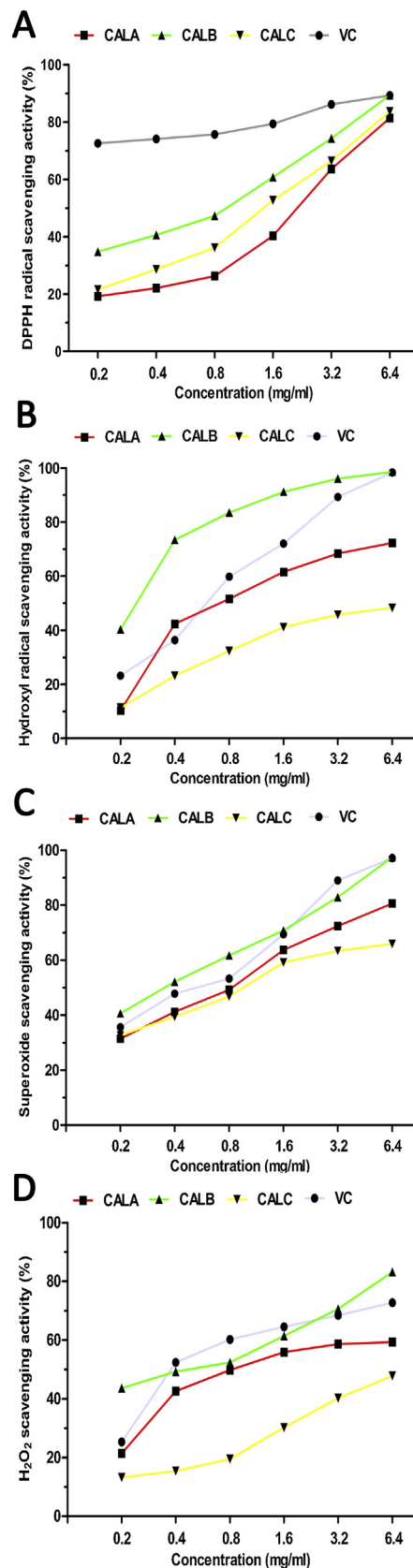


Fig. 4. Scavenging effects on of CALA, CALB, CALC, and VC against (A) DPPH, (B) hydroxyl radicals, (C) superoxide, and (D) H<sub>2</sub>O<sub>2</sub>.

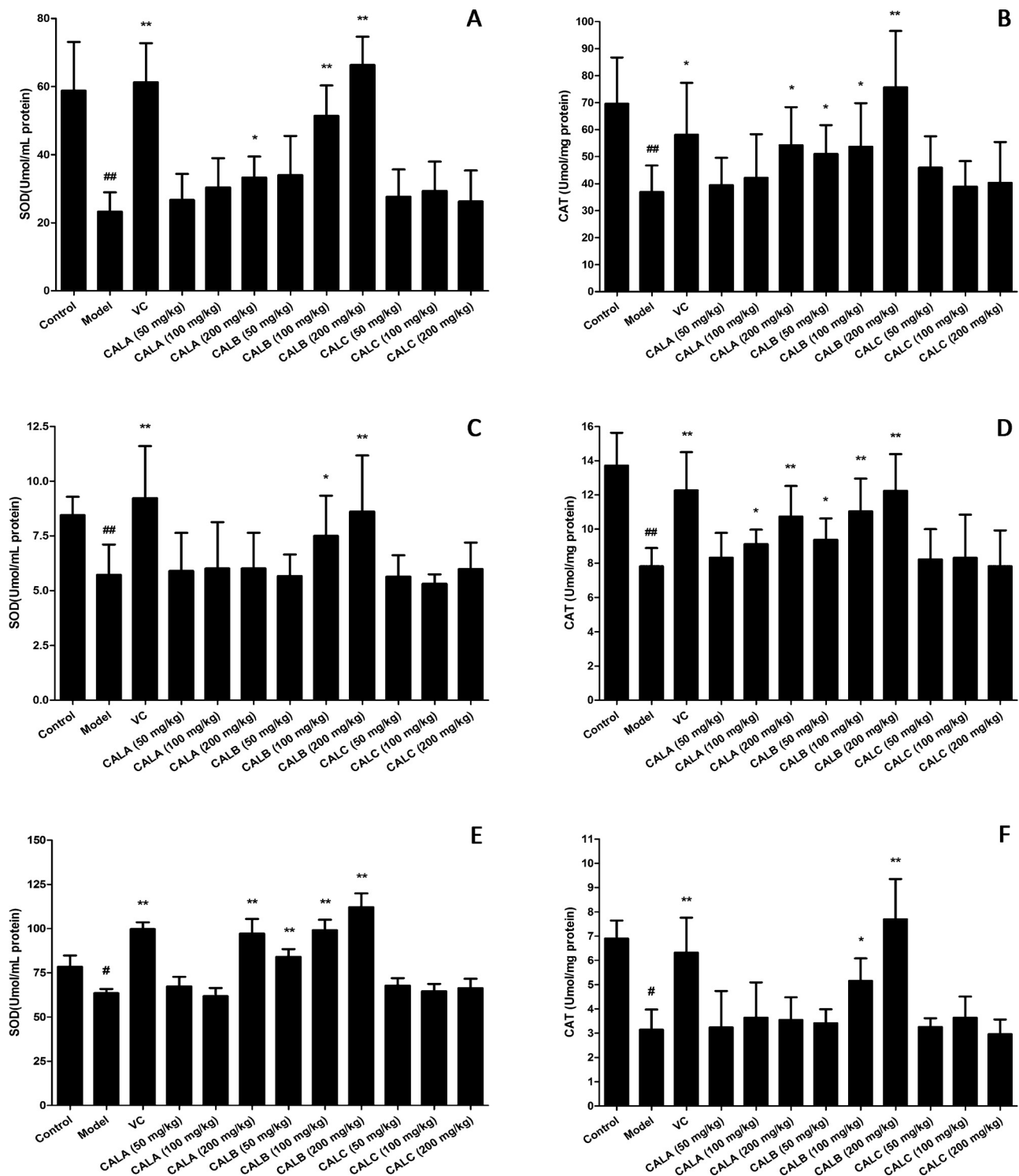


Fig. 5. Effects of the three polysaccharide fractions on SOD (A, C, E) and CAT (B, D, F) activities the blood, heart, and liver of D-galactose-induced aging mice.

CALB, CALC, and VC were 81.4%, 89.4%, 83.7%, and 89.3%, respectively.

**3.6.1.2. Hydroxyl radical scavenging activity.** The hydroxyl radical is a powerful oxidant that can react with nearly all biological molecules, such as carbohydrates, proteins, and lipids. Moreover, oxidative stress can mediate a wide variety of degenerative processes and diseases. As shown in Fig. 4B, the strength of the scavenging effect of CALA, CALB, and CALC correlated with

polysaccharide concentration. Compared with CALA (72.3%), CALC (48.3%) and VC (98.4%), the scavenging effect of CALB (98.6%) was strongest at  $6.4 \text{ mg mL}^{-1}$ .

**3.6.1.3. Superoxide radical scavenging activity.** The superoxide radical is one of the precursors of singlet oxygen and the hydroxyl radical. Superoxide radical indirectly initiates lipid peroxidation. Superoxide radicals can be generated by pyrogallol autoxidation. Fig. 4C shows the scavenging activity of CALA, CALB, CALC, and VC



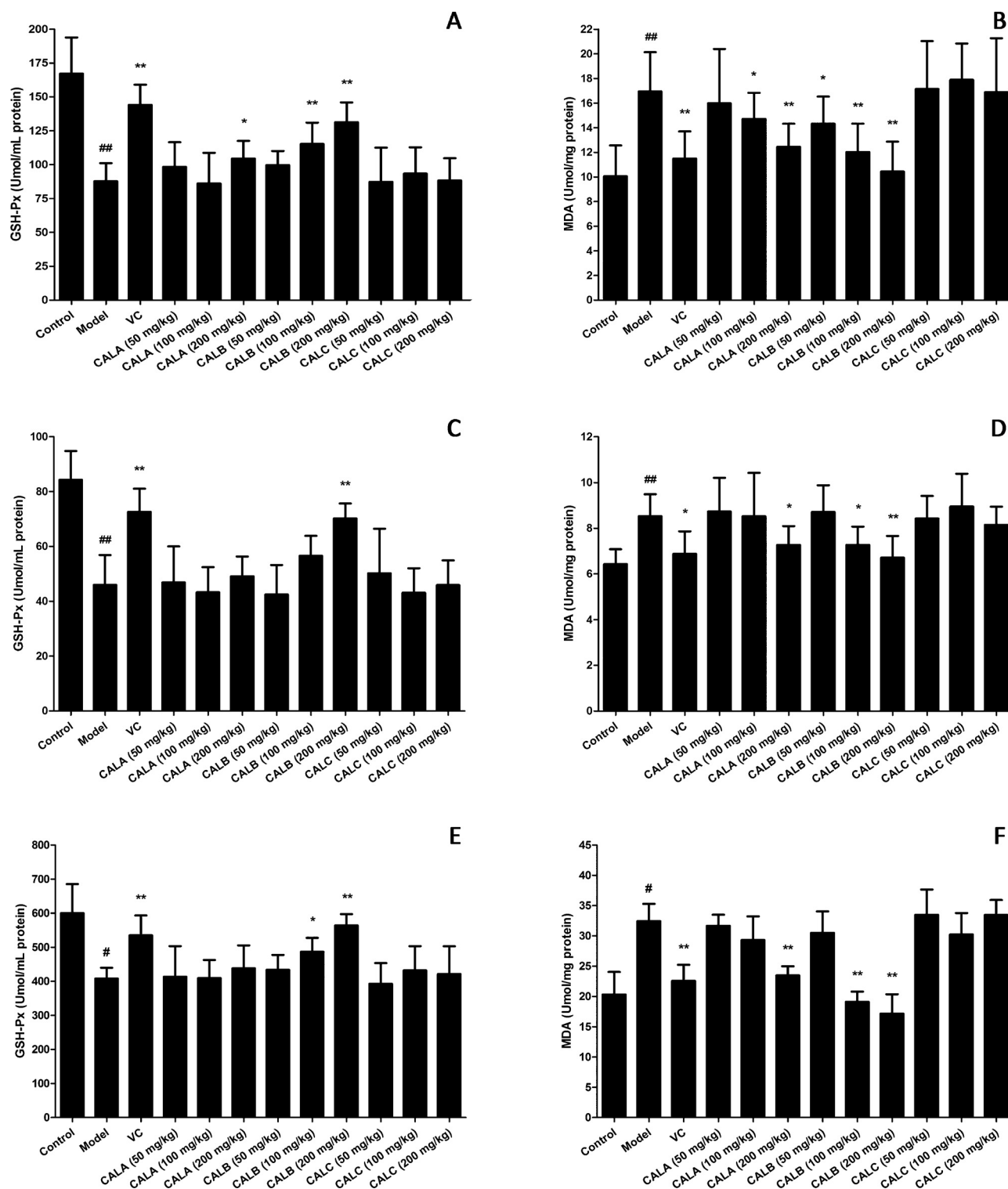


**Fig. 6.** Effects of the three polysaccharide fractions on GSH-Px (A, C, E) activity as well as MDA (B, D, F) content of the blood, heart, and liver of D-galactose-induced aging mice.

at different concentrations against superoxide radicals. The scavenging activity was 97.4% for CALB but only 80.6% and 65.9% for CALA and CALC at  $6.4 \text{ mg mL}^{-1}$ .

**3.6.1.4.  $\text{H}_2\text{O}_2$  scavenging activity.** Fig. 4D shows the scavenging activities of CALA, CALB, CALC, and VC against the  $\text{H}_2\text{O}_2$  radical. The scavenging effects of the three polysaccharides were evident at all tested concentrations. CALB had a stronger scavenging effect than VC and the two other polysaccharides (CALA and CALC) had weaker

activities than VC. At  $6.4 \text{ mg mL}^{-1}$ , the scavenging activities of CALA, CALB, CALC, and VC were 59.3%, 83.2%, 47.8%, and 72.7%, respectively. CALB exhibited the strongest scavenging activity against the  $\text{H}_2\text{O}_2$  radical.

### 3.6.2. Antioxidative activities in vivo

Free radicals and peroxides are involved in numerous physiological processes, such as the pathogenesis of various diseases and the

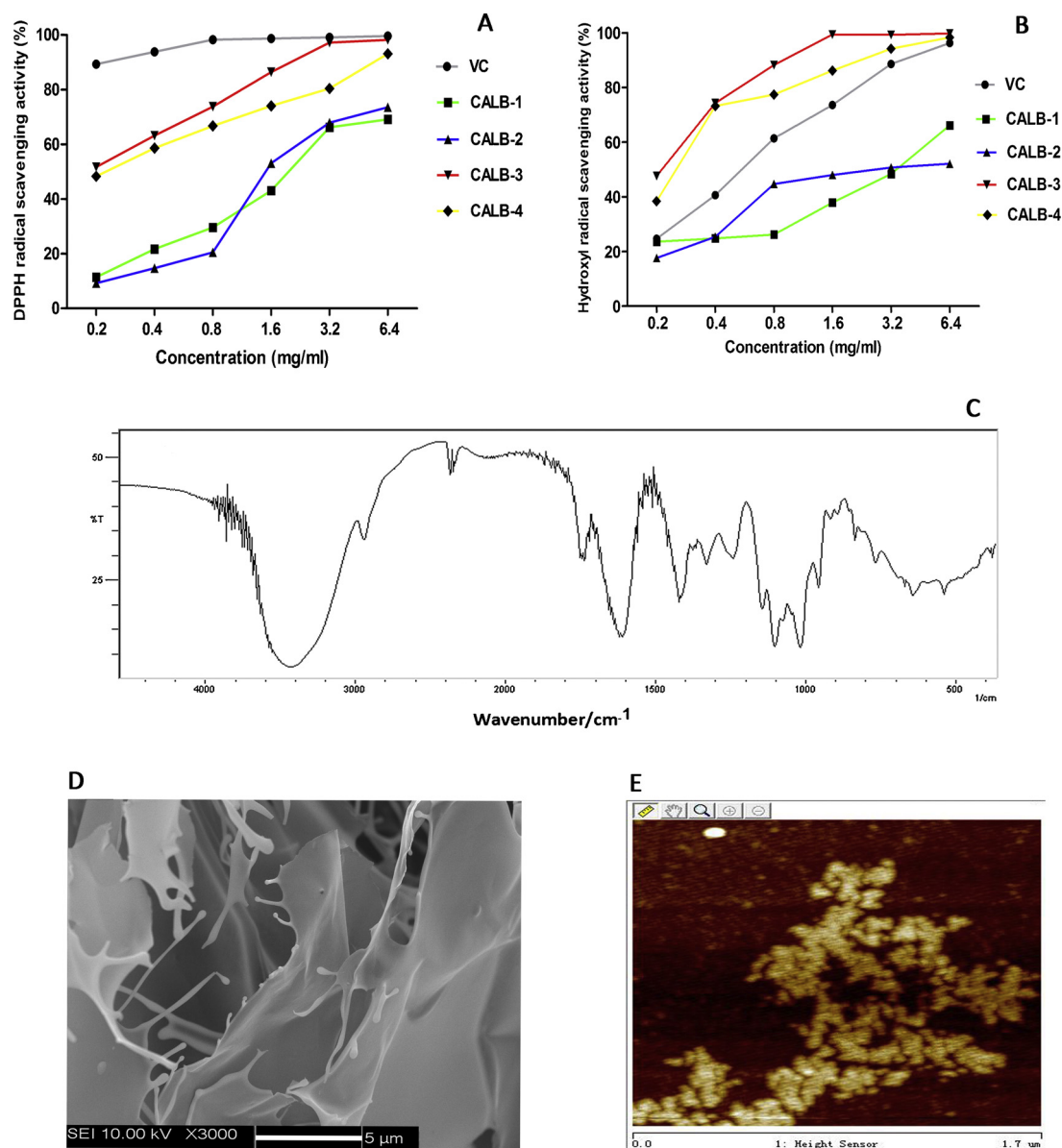


**Fig. 7.** Scavenging effects on of CALB-1, CALB-2, CALB-3, CALB-4, and VC against (A) DPPH and (B) hydroxyl radicals. (C) The IR spectra of CALB-3, recorded in KBr tablet at the absorbance mode from 4000 to 400  $\text{cm}^{-1}$  (midinfrared region) at a resolution of 4  $\text{cm}^{-1}$ . (D) SEM images of CALB-3 at 3000 $\times$ . The molecular morphology of CALB-3 was first coated with a thin layer of gold, then observed using SEM at an accelerating voltage of 10 kV. (E) AFM image of CALB-3. CALB-3 was dissolved in distilled water at the concentration of 5 g/mL. 5 L of solution was dropped onto freshly cleaved mica and allowed to stand in air before imaging.

aging process [17,18]. These biological effects of free radicals and peroxides are generally controlled in vivo by a wide spectrum of antioxidative defense mechanisms [19]. In these mechanisms, the endogenous antioxidant enzymes SOD, CAT, and GSH-Px may limit the levels of reactive oxidants and the damage they inflict on the antioxidant defense system [20]. In the present study, the effects of the three extracted polysaccharides on the activity of endogenous antioxidant enzymes and the level of lipid peroxidation in blood, heart, and liver were investigated in D-galactose-induced aging mice. In the model group (Figs. 5 and 6), almost all SOD, CAT, and GSH-Px enzyme activities in the blood, heart, and liver were significantly decreased compared with the normal group ( $P < 0.05$  or  $< 0.01$ ). Compared with the model group, CALB evidently enhanced the enzyme activities of SOD, CAT, and GSH-Px in blood, heart, and liver, whereas CALA enhanced only SOD, CAT, and GSH-Px activity in blood (Figs. 5, 6A, C, and E). CALC showed no effect in blood, heart, and liver. MDA, a by-product of arachidonate metabolism, was produced because of oxidative cellular damage. Moreover,

MDA resulting from tissue injury can combine with the free amino groups of proteins, producing MDA-modified protein adducts [21]. As shown in Fig. 6B, D, and F, CALA (200 mg/kg) and CALB (100 and 200 mg/kg) significantly reduced MDA formation in blood, heart, and liver compared with the aging model group.

### 3.7. DPPH and hydroxyl radical scavenging activities of four purified polysaccharides

DPPH and hydroxyl radical scavenging activity was performed to evaluate the antioxidant capacity in the presence of various concentrations of CALB-1, CALB-2, CALB-3, and CALB-4. CALB-1 and CALB-2, particularly at doses from 0.2  $\text{mg mL}^{-1}$ , exhibited relatively weak scavenging effects against both DPPH and hydroxyl free radicals compared with CALB-3 and CALB-4. For these two free radicals, CALB-3 and CALB-4 have a more superior scavenging activity than the positive control VC. As shown in Fig. 7A and B, CALB-3 had a stronger scavenging effect on DPPH and hydroxyl free radicals

than CALB-1, CALB-2, and CALB-4. At 6.4 mg mL<sup>-1</sup>, the scavenging activity of CALB-3 was 98.7% and 99.8%, respectively.

### 3.8. FTIR spectra analysis

The IR spectrum of CALB-3 (Fig. 7C) showed a strong band at 3446.56 cm<sup>-1</sup> which was attributed to the hydroxyl stretching vibration of the polysaccharide. The band at 2937.39 cm<sup>-1</sup> was due to C–H stretching vibration. Bands at 1743.53 and 1618.17 cm<sup>-1</sup> indicated the ester carbonyl (COOR) groups and carboxylated ion groups (COO<sup>-</sup>). The FTIR spectrum of CALB-3 showed a strong absorbance at 1074.27 and 1110.92 cm<sup>-1</sup> attributed to the stretching vibrations of  $\alpha$ -pyranose ring of the glucosyl residue. Moreover, the characteristic absorptions at 894.91 and 954.70 cm<sup>-1</sup> indicated that both  $\alpha$ - and  $\beta$ -configurations existed. These observations confirmed that the CALB-3 was a polysaccharide containing uronic acid.

### 3.9. Molecular morphology of CALB-3

Its molecular morphology was further investigated by SEM and AFM. CALB-3 appeared as loose flaky and curly aggregation (Fig. 7D). The observed irregular microstructure demonstrated that CALB-3 was a type of amorphous solid. The molecular morphology of CALB-3 was further investigated by single molecular AFM (Fig. 7E). The results showed that there were many spherical lumps which suggested molecular aggregation happened somehow. There might be a repulsive force between the polysaccharide and the mica causing aggregation because both CALB-3 and the mica a type of aluminum silicate were negative [22]. The side chains might be another reason for the aggregation.

## 4. Discussion

Oxidative stress plays a pivotal role in the pathogenesis of cardiovascular diseases, including ischemia/reperfusion injury, ischemic heart disease, and heart failure [23]. *Zhi-qiao* has been used for more than 2000 years as a common medicine in the treatment of heart disease. So far, only polymethoxylated flavones and flavonoid glycosides have been identified as bioactive compounds with anti-oxidative properties. In the present study, CALB was found to possess significant antioxidant activity in four free radical scavenging tests in vitro and the expression levels of antioxidant enzymes and MDA in mice. Four polysaccharides were purified and isolated from CALB, among which, CALB-3 showed the strongest in vitro antioxidant activity.

A typical mouse model of aging, induced by D-galactose, was used to further evaluate the defensive antioxidant effects of three polysaccharide fractions in vivo. D-Galactose, as a reducing sugar, is involved in three metabolic pathways. Rodents chronically injected with D-galactose have disturbed carbohydrate metabolism in the body, resulting in the formation of end-products in vivo with advanced glycation [24]. Simultaneously, D-galactose also stimulates free radical generation and accumulation via a galactose-oxidase metabolic pathway, thus resulting in oxidative stress to the body [25]. By detecting the activity of SOD, CAT, and GSH-Px, as well as MDA content, we found that only CALB demonstrated stronger antioxidant activity in vivo, whereas CALC showed no effect. Although three of the polysaccharides were shown to have roles in the scavenging free radicals in vitro test, the scavenging effect of CALB was strongest compared with CALA and CALC. The results indicated that acidic polysaccharides might have no effects in vivo antioxidant test.

Next we investigated the structural characteristics, including differences, of the three polysaccharide fractions. Preliminary

structural characterizations of their physicochemical properties were conducted and analysis using FTIR and SEM was performed. These analyses demonstrated that the basic physicochemical property of the three polysaccharides were similar, however the SEM images revealed that the different extraction methods produced different stereostructures.

In order to further study the relationship between the polysaccharide structures and their antioxidant activities, four purified polysaccharides were isolated from CALB, among which CALB-3 showed the strongest antioxidant activity against DPPH and hydroxyl in vitro. It has been reported that many factors affect the activities of polysaccharides, including monosaccharide composition, molecular mass, glycosyl residues, and chain conformation [26]. Analysis of the monosaccharide composition of the four purified polysaccharides demonstrated that CALB-3 and CALB-4 mainly consist of the neutral sugars Man, Rha, Gal, and Ara (92.2% and 83.7%), with small amounts of the acidic sugars GlcUA and GalUA (7.8% and 16.3%, respectively). Acidic monosaccharides of CALB-1 and CALB-2 accounted for almost half of the total sugar content. CALB-3 and CALB-4 exhibited greater antioxidant effects than CALB-1 and CALB-2, and this may be due to their higher neutral sugar content. Using SEM and AFM, we found that CALB-3 appeared to be aggregated in spherical lumps. This aggregation may also underlie the antioxidant activity. In addition, we found that CALB-3 had myocardial protective effects via improved free radical scavenging and antioxidant activity, however further work is needed to identify the detailed mechanism. We therefore conclude that monosaccharide composition and aggregation are extremely important in the biological activities of CALB-3, and that further studies are needed to elucidate the structure–function relationships and mechanisms responsible for its antioxidant activities.

## 5. Conclusion

Finally, based on the results we observed, CALB and CALB-3 may be novel safe antioxidant candidates. This finding extends our understanding of the effects of *C. aurantium* L. and its polysaccharide components. In order to promote our research and the development of CALB and CALB-3 and establish the therapeutic potential for the prevention and treatment of heart disease, further investigations will focus on the mechanism of myocardial protection by CALB and CALB-3.

## Acknowledgment

The Major State Basic Research Development Program of China (973 Program 2013CB531800).

## References

- [1] H.J. Zhang, Y.Y. Cheng, *Biomed. Chromatogr.* 20 (2006) 821–826.
- [2] W. He, Y. Zhang, X. Wang, L. Guo, L. Han, E. Liu, T. Wang, *J. Med. Food* 16 (2013) 306–311.
- [3] M. Kang, J.H. Kim, C. Cho, H.S. Chung, C.W. Kang, Y. Kim, M. Shin, M. Hong, H. Bae, *J. Ethnopharmacol.* 111 (2007) 584–591.
- [4] S. Jia, F. Li, Y. Liu, H. Ren, G. Gong, Y. Wang, S. Wu, *Int. J. Biol. Macromol.* 62 (2013) 66–69.
- [5] I.A. Schepetkin, M.T. Quinn, *Int. Immunopharmacol.* 6 (2006) 317–333.
- [6] H.P. Han, H.C. Xie, *Afr. J. Tradit. Complement Altern. Med.* 10 (2013) 485–489.
- [7] X.Y. Men, W.G. Xu, X. Zhu, W.C. Ma, *Zhong Yao Cai* 32 (2009) 1891–1894.
- [8] J. Zhang, Y. Lu, D. Chen, *Zhongguo Zhong Yao Za Zhi* 37 (2012) 2071–2075.
- [9] J.A. Batista, E.G. Dias, T.V. Brito, R.S. Prudêncio, R.O. Silva, R.A. Ribeiro, M.H. Souza, R.C. de Paula, J.P. Feitosa, L.S. Chaves, M.R. Melo, A.L. Freitas, J.V. Medeiros, A.L. Barbosa, *Carbohydr. Polym.* 99 (2014) 59–67.
- [10] H.X. Kuang, X.G. Xia, B.Y. Yang, Q.H. Wang, Y.H. Wang, *Carbohydr. Polym.* 83 (2011) 787–795.
- [11] X.M. Yang, W. Yu, Z.P. Ou, H.L. Ma, W.M. Liu, X.L. Ji, *Plant Food Hum. Nutr.* 64 (2009) 167–173.
- [12] K. Elizabeth, M.N.A. Rao, *Int. J. Pharm.* 58 (1990) 237–240.

- [13] K. Deepalakshmi, S. Mirunalini, M. Krishnaveni, V. Arulmozhi, *Chin. J. Nat. Med.* 11 (2013) 621–627.
- [14] İ. Gülçin, *Arch. Toxicol.* 86 (2012) 345–391.
- [15] D.B. Ji, J. Ye, C.L. Li, Y.H. Wang, J. Zhao, S.Q. Cai, *Phytother. Res.* 23 (2009) 116–122.
- [16] R. Gnanasambandam, A. Proctor, *Food Chem.* 68 (2000) 327–332.
- [17] L. Aksoy, E. Kolay, Y. Ağılönü, Z. Aslan, M. Kargioğlu, *Saudi J. Biol. Sci.* 20 (2013) 235–239.
- [18] R. Pandey, S. Gupta, V. Shukla, S. Tandon, V. Shukla, *Indian J. Exp. Biol.* 51 (2013) 515–521.
- [19] K.H. Musa, A. Abdullah, B. Kuswandi, M.A. Hidayat, *Food Chem.* 141 (2013) 4102–4106.
- [20] X. Sun, G.B. Sun, M. Wang, J. Xiao, X.B. Sun, *J. Cell Biochem.* 112 (2011) 2019–2029.
- [21] R. Stocker, J.F. Keaney, *Physiol. Rev.* 84 (2004) 1381–1478.
- [22] M. Sletmoen, G. Maurstad, P. Sikorski, B.S. Paulsen, B.T. Stokke, *Carbohydr. Res.* 338 (2003) 2459–2475.
- [23] D.P. Pandya, *Compr. Ther.* 27 (2001) 284–292.
- [24] X. Song, M. Bao, D. Li, Y.M. Li, *Mech. Ageing Dev.* 108 (1999) 239–251.
- [25] X. Cui, L. Wang, P. Zuo, Z. Han, Z. Fang, W. Li, J. Liu, *Biogerontology* 5 (2004) 317–325.
- [26] X.F. Bao, C.P. Liu, J.N. Fang, X.Y. Li, *Carbohydr. Res.* 332 (2001) 67–74.